UNIVERSITY OF TURIN

DOCTORAL SCHOOL IN LIFE AND HEALTH SCIENCES

PhD PROGRAMME IN

EXPERIMENTAL MEDICINE AND THERAPY

XXXII CYCLE

PhD PROGRAMME CO-ORDINATOR

Prof. Pasquale Pagliaro

PhD THESIS

CHARACTERIZATION OF ANTERIOR MEDIASTINAL TUMOURS COMBINING MOLECULAR IMAGING AND PERFUSION IMAGING THROUGH DIFFUSION-WEIGHTED AND DYNAMIC CONTRAST-ENHANCED MAGNETIC RESONANCE

SUPERVISOR

Prof. Andrea Veltri

PhD STUDENT

Adriano Massimiliano Priola

Department of Radiology, San Luigi Gonzaga Hospital, University of Turin, Orbassano (To), Italy

Abstract

Introduction:

Diffusion-weighted (DW) magnetic resonance (MR) and dynamic-contrast enhanced (DCE)-MR are helpful in tissue characterization in different organs and compartments, and provide quantitative or semi-quantitative data, in addition to morphological assessment, in order to improve diagnostic performance of MR. The aim of our prospective study was to evaluate their ability in distinguishing different conditions and tumours of the anterior mediastinum.

Materials and Methods:

In the period study, 49 patients with an anterior mediastinal lesion or tissue detected on computed tomography, who obtained histological diagnosis, were enrolled. DW-MR and DCE-MR of the anterior mediastinum were performed. Two radiologists analyzed MR imaging by calculating the ADC on ADC-map and by reconstructing the time-signal intensity curve (TIC), both obtained with dedicated software, of the solid tissue in the anterior mediastinum. About TIC of DCE-MR, time to peak (TTP) was defined as the time of the signal intensity peak from contrast-medium injection and wash-out ratio (WOR) was calculated. Based on TTP and WOR, the TIC was categorized as persistent pattern (TTP>120s), plateau pattern (TTP≤120s, WOR≤30%) and washout pattern (TTP≤120s, WOR>30%). In addition, semi-quantitative data derived from TIC (e.g., wash in ratio (WIR), area under the curve (AUC), and maximum enhancement ratio (MER)) were obtained.

Results:

The inter-reader agreement was excellent for all quantitative parameters (ICC>0.8). Concerning DW-MR, lymphoid thymic hyperplasia (LTH) had the highest ADC values compared to all mediastinal tumours grouped in a single group (mean, $1.86x10^{-3}mm^2/s$ versus $1.20x10^{-3}mm^2/s$; $p<0.0001$) and compared to each different type of tumour, although overlapped ADC values were found between LTH and non-advanced thymomas (stage I and II, Masaoka-Koga staging system) in 11 cases (6 thymomas, 4 LTH) in the range from 1.61 to $1.77x10^{-3}mm^2/s$. Notably, among tumours,

thymoma showed higher ADC values (mean, $1.26x10^{-3}mm^2/s$) compared to thymic carcinoma and lymphoma (mean, 0.98 and $1.15x10^{-3}mm^2/s$, respectively), although no significant differences in ADC values were found between different tumour groups. Concerning DCE-MR, all cases but one of LTH and 80% (12/15 cases) of lymphomas showed a plateau pattern on TIC, whereas the washout pattern was seen only in thymic epithelial tumours (6/22 cases, 27%), which included 2 out of 3 (66%) thymic carcinomas and four thymomas (all high grade thymomas based on Jeong histological classification). Notably, for thymic epithelial tumours, the plateau pattern was seen in 3 out of 22 cases (14%) of thymomas (all low grade thymomas) and in no case of thymic carcinoma. TIC pattern was able to discriminate LTH and lymphoma from thymic epithelial tumours ($p<0.001$). In addition, for differentiating thymomas from lymphomas by using semi-quantitative data from TIC, significant different mean values were found for WIR (16.1 versus 28.8 a.u./s, respectively; $p=0.0001$), AUC (157 versus $265x10^3$; $p=0.0014$), and MER (145.0 versus 222.0; $p<0.0001$). The ROC analysis showed that the MER had the best diagnostic performance in this discrimination (area under the ROC curve, 0.877; sensitivity, 87%; specificity, 79%). Lastly, MER and WIR were found useful in discriminating thymic epithelial tumours from lymphomas.

Conclusion:

By using ADC, DW-MR is useful in differentiating LTH from anterior mediastinal tumours although overlapped ADC values can be found between LTH and low grade thymomas. Furthermore, it is not able to distinguish between thymic epithelial tumours and lymphomas. However, DCE-MR has additional value in discriminating between different tumours of the anterior mediastinum, namely thymic epithelial tumours and lymphomas, by analysing the TIC pattern and by using some semi-quantitative parameters obtained from TIC.

Text

Introduction

In the characterization of lesions located in the anterior mediastinum, computed tomography (CT) is generally the first choice modality of diagnostic imaging, although in the last fifteen years thoracic magnetic resonance (MR) has become a promising tool by using conventional T1- and T2-weighted spin echo imaging for evaluating the anatomical detail because of its better soft-tissue contrast compared to CT (Ackman JB, 2014; Raptis CA, 2018). Indeed, in clinical practice, for the evaluation of the anterior mediastinum, the use of MR has considerably increased, by acquiring conventional and functional imaging, due to technological improvements and standardization of thoracic protocols (Ackman JB, 2011; Ackman JB, 2015). Currently, MR imaging is increasingly seen as an useful problem-solving modality, especially in equivocal cases at CT, with the advantage of a higher contrast resolution and no radiation exposure. For example, the use of conventional T2-weighted sequences easily allows discrimination between dense cysts on CT examination (cysts with CT attenuation greater than 20 Hounsfield Units) and homogeneous solid mediastinal tumours, such as low-grade thymomas without calcifications (Ackman JB, 2014; Ackman JB, 2015). In addition, by detecting microscopic fat in tissue, chemical-shift MR imaging is useful for differentiating normal thymus and rebound thymic hyperplasia from cancer tissue at diagnosis and after chemotherapy in oncologic patients, and for distinguishing lymphoid thymic hyperplasia (LTH) from thymoma in autoimmune diseases such as myasthenia gravis (Takahashi K, 2003; Inaoka T, 2005; Nishino M, 2006; Inaoka T, 2007; Priola AM, 2015).

Diffusion-weighted (DW)-MR is another useful tool for characterizing normal thymus and thymic abnormalities or mediastinal lesions, by reflecting tumour cell density and cellular architecture (Ackman JB, 2014; Priola AM, 2016). Nowadays, DW-MR is usually included in the standard protocol for the detection and characterization of mediastinal tumours, for their differentiation from benign conditions and in monitoring the response to chemotherapy (Padhani AR, 2009; Abdel

Razek AAK, 2012; Ackman JB, 2014; Ackman JB, 2015; Abdel Razek AAK, 2015; Priola AM, 2016; Priola AM, 2018). The intra- and extracellular molecular diffusion of water detected by DW-MR, that is sensitive to thermally drive molecular water motion, can be measured as signal loss and expressed with the apparent diffusion coefficient (ADC). The ADC depends largely on the presence of barriers to diffusion within the water microenvironment, namely cell membranes and macromolecules, that alter the diffusion characteristics of the tissue (Padhani AR, 2009). On this basis, DW-MR has been used in different organs to differentiate benign from malignant lesions. Benign lesions (as LTH) usually present high ADC values and unrestricted diffusion, whereas malignant lesions (as thymic epithelial tumours or lymphomas) have low ADC values and restricted diffusion (Padhani AR, 2009; Abdel Razek AAK, 2012; Abdel Razek AAK, 2015; Priola AM, 2016; Priola AM, 2018). In clinical setting, quantitative DW-MR through the measurement of ADC is particularly useful in differentiating normal thymus from lymphoma of the anterior mediastinum in young patients (who can have non-suppressing normal thymus at chemical-shift MR because of the absence of detectable fatty component within the thymus) or non-suppressing LTH at chemical-shift MR from thymoma in young subjects with new onset of myasthenia gravis. It is also helpful in discriminating malignant lymph nodes from benign ones (e.g., sarcoidosis) which are characterized by normal diffusion of water molecules with high ADC values (Abdel Razek AAK, 2012; Gumustas S, 2012; Gumustas S 2013; Priola AM, 2015; Priola AM, 2018). However, at present, no studies showed significant differences in ADC values between thymomas or thymic epithelial tumours and lymphomas, which represent overall most of tumours in the anterior mediastinum (Abdel Razek, 2009; Yabuuchi H, 2015; Priola AM, 2016). Furthermore, in the evaluation of patients with myasthenia gravis, previous studies found overlapped ADC values between normal thymus or LTH and low grade thymomas (type A, AB, B1 according to the WHO histological classification of thymic epithelial tumours) or non-advanced thymomas (stage I and II according to the Masaoka-Koga surgical classification) which are not characterized by significant cellular abnormalities. Thus, in some cases, these tumours may not present restriction on free diffusion of

water molecules, as usually seen in normal thymus and thymic hyperplasia (Priola AM, 2015). Therefore, the ADC may have limits in the evaluation of the anterior mediastinum.

Dynamic contrast-enhanced (DCE)-MR evaluates the degree of contrast enhancement of a biological tissue over time, providing information regarding changes in perfusion of the tissue which are based on the time-signal intensity curve (TIC) that defines the wash-in and wash-out enhancement of the tissue (Coolen J, 2012). DCE-MR, even in association with DW-MR, has proven useful in characterizing malignant lesions in different organs and compartments (e.g., brain, breast, and testicle), including the thorax (lung and pleura) (Coolen J, 2012; Coolen J, 2015; Liu HL, 2018; Manganaro L, 2018). About the anterior mediastinum, the usefulness of DCE-MR has been evaluated in two different studies: the former (Sakai S, 2002) investigated the effectiveness of DCE-MR in the differentiation of thymomas from other tumours (mostly thymic carcinomas and lymphomas) in 49 patients through the analysis of different TIC patterns and the evaluation of time to peak (TTP, which is the time to reach the enhancement peak from contrast medium administration); the latter (Yabuuchi H, 2015) assessed the reliability of DCE-MR, in association with DW-MR and FDG-PET/CT, in the distinction between thymic epithelial tumours and lymphomas/germ cell tumours through the analysis of TIC morphology on the basis of three distinct patterns ("persistent", "plateau", "washout") which are defined by the TTP and the wash-out ratio (WOR) of the TIC. However, these studies on DCE-MR of the anterior mediastinum have some limitations. Firstly, they are based on morphological characteristics of TIC which was obtained by using only two semi-quantitative data (TTP, WOR). Thus, they do not use additional semi-quantitative parameters derived from TIC (e.g., wash-in ratio (WIR), area under the curve (AUC), maximum enhancement ratio (MER), peak enhancement (PE)) which have proved useful in the characterization of tumours and in their differentiation from benign conditions in other compartments, such as breast, pleura, and testicle (Liu HL, 2018; Coolen J, 2012; Manganaro L, 2018).

The aim of the present study was to prospectively evaluate the utility of DW-MR and DCE-MR in the characterization of mediastinal abnormalities, through the measurement of the ADC for DW-MR and by evaluating the TIC pattern and semi-quantitative parameters obtained from TIC for DCE-MR. In particular, we investigated the ability of DW-MR and DCE-MR in the differentiation between thymic epithelial tumours and lymphomas, as well as between mediastinal tumours and non-suppressing LTH at chemical-shift MR (i.e., thymic hyperplasia with no signal intensity loss on "opposed-phase" imaging compared to "in-phase" imaging because of the insufficient amount of microscopic fat within the thymus).

Materials and Methods

Patient Population and Reference Standard

An institutional review board approved the study, and written informed consent was obtained. From March 2014 through September 2020, all subjects who underwent CT of the chest with detection of abnormalities of the anterior mediastinum were considered eligible for inclusion. Subjects with myasthenia gravis and a thymus within the limit of normal for a given patient's age at CT, that could be a non-enlarged LTH, were also included. All subjects with CT findings suggestive for a normal thymus were excluded. Other exclusion criteria in patients with abnormal CT scans were contraindications to MR (e.g. cardiac pacemaker, claustrophobia, contraindication to administration of contrast medium) and patient refusal to enrolment. All CT scans were evaluated by one radiologist, with more than 14 years of experience in thoracic CT, that enrolled all subjects. Thus, in the study period, we prospectively enrolled 49 consecutive subjects, 22 men and 27 women (mean age, 47.4±20.8 years; range, 15-82 years; median age, 49 years; interquartile range, 27-64 years). All patients were grouped on the basis of histological diagnosis which was obtained for all subjects by the use core biopsy and mediastinoscopy (tumour group including lymphoma, lymph node metastasis, germ cell tumour, some cases of thymic epithelial tumours), or surgical removal through extended thymectomy (benign group of LTH) or thymomectomy (tumour group including remaining cases of thymic epithelial tumours) of the anterior mediastinal tissue. For LTH group in

patients with newly diagnosed generalized myasthenia gravis, all thymuses with soft-tissue attenuation and non visible fat on CT were selected. On chemical-shift MR, the radiologist selected all subjects with non-suppressing thymus, by visually analyzing in-phase and opposed-phase imaging, who subsequently underwent extended thymectomy.

MR Imaging Protocol

All MR examinations were performed with a 1.5-T unit (Intera-Achieva, Philips Healthcare, Best, The Netherlands) using a 16-channel phased-array surface coil. Pulse sequence parameters of T2-weighted single-shot spin-echo echo-planar DW-MR and T1-weighted three-dimensional gradient-echo DCE-MR are detailed in **Table 1**. DCE-MR was performed in the selected field of view before, during, and after a bolus intravenous injection of 7 ml of gadolinium (Multihance, Bracco) at a rate of 2 ml/s (total dose, 0.1 mmol/kg of body weight) by using an automatic power injector, followed by a 20 ml saline flush. This sequence was repeated 23 times every 20 seconds with a total imaging time acquisition of 8 minutes.

For all patients, the MR protocol also included T2-weighted single-shot turbo spin-echo imaging without and with fat suppression (repetition time/Echo time, 386/100 and 415/80 ms, respectively; matrix, 224 x 224; section thickness/intersection gap, 5/0 mm) and T1-weighted dual gradient-echo chemical-shift imaging in the same breath hold with the following imaging parameters: 240-400 mm field-of-view, 256x256 image-matrix, 5-mm section-thickness, 0-0.5 mm intersection-gap, flip-angle 90^0, repetition-time 154 ms, and in-phase and opposed-phase echo-times of 4.6 and 2.3 ms. An anterior-to-posterior phase-encoding direction was used on the in-phase and opposed-phase images. This frequency encoding direction was preferred over the right-to-left or left-to-right phase-encoding direction in order to avoid or minimize the presence of artifacts within the anterior mediastinum (chemical-shift of the first kind or spatial misregistration) at the lipid-water interface between the hyperplastic thymus or the anterior mediastinal mass on one hand, and the great vessels or the chest wall on the other (Inaoka T, 2007).

The entire tumour or tissue of the anterior mediastinum was included in MR examination.

MR Image Analysis

Two radiologists (14 and 3 years of experience in thoracic MR, respectively), who were blinded to patients' data and histological diagnoses, independently analyzed each exam for qualitative (TIC pattern), quantitative (transverse diameter, signal intensity index (SII) of chemical-shift MR, ADC) and semi-quantitative (parameters obtained from the TIC curve) assessment by using a Windows workstation with dedicated software (Extended MR Work-Space, v. 2.6.3.1; Philips Healthcare). The longest diameter of the lesion or tissue was measured at the widest dimension on transverse cross-sectional images. T2-weighted MR with fat suppression was used to detect pure fatty lesions of the anterior mediastinum (i.e. lipomas). Chemical-shift MR imaging was used to detect patients with normal thymus and lymphoid or rebound thymic hyperplasia with evident fat tissue, who were excluded from the study, by demonstrating the decrease in signal intensity of the thymus gland on the opposed-phase images relative to the in-phase images on qualitative assessment. For cases of non-suppressing LTH (i.e., no signal loss at visual assessment on opposed-phase chemical-shift imaging), the SII was measured in order to exclude cases with SII equal or greater than 8.62% (Priola AM, 2015). The SII was obtained by positioning an electronic cursor, using regions of interest (ROI) of the same size, that was placed over the same position within the tissue on both in-phase and opposed-phase images in each case. The selection of the ROI placement was first made on the opposed-phase image, in order to avoid the inclusion of areas of signal void at the interfaces between the fat-dominant and water-dominant tissues (India ink artifact), and then mirrored on the in-phase image in the exact same position. On the opposed-phase T1-weighted image, the readers placed the ROI on the anterior mediastinal soft tissue that exhibited the highest signal intensity, avoiding cystic, necrotic, or calcified components. The SII of the thymus and lesions was calculated as $[(tSI_{in}–tSI_{op})/(tSI_{in})]x100\%$ (t, thymus; in, in-phase imaging; op, opposed-phase imaging).

For quantitative assessment of DW-MR, both readers reconstructed the ADC-maps from the *b* of 150, 500, and 800 s/mm^2 images for suppressing tissue perfusion (included at *b* values less than 100 s/mm^2) in order to obtain perfusion-free ADC values (Padhani AR, 2009; Priola AM, 2016). For

each patient, all the axial sections which included the tumour or tissue were identified and within three of these sections, with largest areas of restriction on ADC-maps, a region of interest (ROI) was defined using an electronic cursor along the circumference of the tissue, but within the boundaries. The ROI was manually drawn to include only the solid portion of the tissue, taking care to exclude obvious cystic and/or necrotic areas (which could give falsely elevated ADC value) that were identified on the corresponding conventional T2-weighted images with and without fat suppression. The mean ADC was calculated from all the ADC values obtained at each axial section of the relative ADC-map for each case and was used for further analyses (Abdel Razek AAK, 2015).

About DCE-MR, colour maps of the dynamic perfusion of the tissue were obtained for each case. Then ROIs were positioned (surface area from 60 to 100 mm^2) within the area of greatest contrast-enhancement in the solid mediastinal tissue, excluding cystic or necrotic areas detected on T2-weighted imaging. A further ROI of similar size was also positioned at the same axial level within the descending thoracic aorta, in order to compare the areas under the curve (AUC) obtained from the perfusion of aorta and mediastinal tissue. The TIC of mediastinal tumour or LTH was obtained with dedicated software and its morphology was evaluated according to the scheme previously proposed by Yabuuchi and collaborators (Yabuuchi H, 2015). In this study, the authors identified free types of TIC based on morphology, TTP, and WOR. In particular, TTP was defined as the time of the signal intensity peak from contrast-medium injection and wash-out ratio (WR) was calculated. Based on these data, the TIC pattern was categorized as persistent pattern (TTP>120s), plateau pattern (TTP≤120, WOR<30%) and washout pattern (TTP≤120, WOR>30%). Semi-quantitative analysis of TIC was subsequently performed, with the evaluation of the following parameters, in addition to TTP and WOR, obtained with dedicated software from TIC:

- wash-in ratio (WIR): obtained by using the formula $(SI_{peak} - SI_0)/TTP$ (a.u./s), considering SI_{peak} as the maximum signal intensity reached by TIC and S_0 as the signal intensity of the pre-contrast imaging;

- wash-out ratio (WOR): obtained by using the formula $(SI_{peak} - SI_0)/(SI_f - SI_0)$ (a.u./s), considering SI_f as the signal intensity at the last point obtained 8 minutes after the administration of Gadolinium along the TIC;

- area under the curve (AUC): the area under the TIC;

- maximum enhancement ratio (MER): obtained by using the formula $(SI_{peak} - SI_0)/SI_0$;

- peak enhancement (PE): considered as the absolute highest signal intensity value along the TIC;

- TIC slope (SI_{slope}): obtained by using the formula $(SI_f - SI_{1-2})/SI_{1-2}$, considering SI_{1-2} as the average value of the first two points on the TIC after administration of Gadolinium;

- early signal enhancement ratio (ESER): obtained by using the formula $(SI_1 - SI_0)/(SI_2 - SI_0)$, considering SI_1 and SI_2 as the signal intensity value at the first and second measuring points of the TIC, respectively, after administration of Gadolinium;

- initial percentage of enhancement ($E_{initial}$): obtained by using the formula $(SI_1 - SI_0)/SI_0$;

- second enhancement percentage (SE_p): obtained by using the formula $(SI_2 - SI_0)/SI_0$;

Statistical Analysis

The Shapiro-Wilk test was used to check the distribution of continuous numeric data. Data with normal distribution were reported as mean values ± standard deviation (SD) and ranges. The median value with interquartile range was added for data with non-normal distribution. The inter-observer agreement was analyzed by calculating the interclass correlation coefficient (ICC) for quantitative data (ICC, range: from 0 - no agreement - to 1 - perfect agreement -). Differences in quantitative data between groups (LTH versus tumours, thymomas versus lymphomas, and thymic epithelial tumours versus lymphomas) and were evaluated by using the *t*-test for equal or unequal variance (Welch *t*-test) after the equality of variance was tested with the *F*-test. For the comparison of the frequency of each TIC pattern on DCE-MR, the chi-square test or Fisher's exact probability test was used to evaluate whether there were any significant differences between LTH, thymic epithelial tumours, and lymphomas. In addition, logistic regression models were estimated in order to evaluate the ability of ADC (in differentiating LTH from mediastinal tumours) and the ability of

semi-quantitative data of DCE-MR (in differentiating thymomas from lymphomas, and thymic epithelial tumours from lymphomas) to discriminate between different conditions of the anterior mediastinum. The discrimination abilities were evaluated by calculating the area under the receiver operating characteristic curve (AUROC), and the optimal cut-off points were individuated according to the Youden index with calculation of sensitivity and specificity. Differences in diagnostic performance of the different semi-quantitative data of DCE-MR were analyzed by comparing ROC curves according to the method proposed by DeLong. Additional analyses that included age and transverse diameter in the logistic models were performed with the aim to control for potential confounders. *P* values less than 0.05 were considered to indicate a statistically significant difference. Analyses were performed using MedCalc (version 15.6.1; MedCalc, Ostend, Belgium).

Results

Patients and histological diagnoses

The demographic characteristics of the study population and the sample size of each group with mean age and transverse diameter are detailed in **Table 2**.

The mean patients' age [SD] in LTH group (32 years [17 years]) and lymphoma group (37 years [21 years]) was significantly lower than that in thymic epithelial tumours group (60 years [14 years) ($p<0.001$). Similarly, significant differences in lesion size were observed between LTH group and lymphoma group ($p<0.001$). The mean lesion size [SD] in thymic epithelial tumours group (63 mm [24 mm]) was significantly higher than that in LTH group (43 mm [15 mm]) and significantly lower than that in lymphoma group (83 mm [17 mm) ($p<0.01$).

About histological diagnosis, according to WHO histological classification, in the thymic epithelial tumours group, the cohort included 1 patient with type A thymoma, 3 type AB, 7 type B1 (therefore 11 low-risk thymomas according to Jeong classification), 3 type B2, 6 type B3 (9 high-risk thymomas), and 3 type C (thymic carcinomas). In the same group, according to the Masaoka-Koga staging system of thymic epithelial tumours, there were 2 stage I thymomas, 8 stage II thymomas

(overall, 10 cases of non-advanced thymomas), 7 stage III (6 thymomas, 1 thymic carcinoma), and 5 stage IV (3 thymomas and 2 thymic carcinomas; overall, 12 advanced thymomas). In stage IV, pleural and/or pericardial implants (stage IVa) or lymph node metastases (stage IVb) were found after surgical resection. In the lymphoma group, most Hodgkin lymphomas (8/11, 73%) were scleronodular ones, while most non-Hodgkin lymphomas (3/4, 75%) were large B cell lymphomas. In the lymph node metastasis group, both patients presented breast cancer with lymph node involvement of the anterior mediastinum. Lastly, in the LTH group, all patients had generalized myasthenia gravis and underwent therapeutic extended thymectomy.

Inter-observer Variability for ADC of DW-MR and DCE-MR semi-Quantitative Parameters

For ADC and semi-quantitative parameters of DCE-MR, the inter-reader agreement between readers was excellent with an ICC greater than 0.8. The lower ICC was found for SEp (ICC=0.823; 95%CI: 0.747-0.880), whereas the higher ICC was found for ADC (ICC=0.969; 95%CI: 0.946-0.983). Therefore, because of the high agreement between the two readers, the mean value of each parameter between the two readers was used for statistical analysis.

At last, perfect agreement was found between the two readers in the evaluation of TIC pattern of DCE-MR, grouped in three types, for all cases (Cohen's k=1).

DW-MR: Differences in ADC between Groups and Subgroups

Table 3 shows the ADC values for all groups and subgroups. By evaluating the two groups with the largest number of subjects (thymic epithelial tumours and lymphomas, 22 and 15 cases, respectively), there were no significant differences in ADC values (thymic epithelial tumours, $1.24x10^{-3}mm^2s^{-1}$; lymphomas, $1.15x10^{-3}mm^2s^{-1}$; p=0.29). The same result was found in the comparison between lymphomas and thymomas (thymomas, $1.28x10^{-3}mm^2s^{-1}$; p=0.12).

The LTH group had significantly higher ADC values compared to all remaining cases grouped in a single tumour group (LTH, $1.86x10^{-3}mm^2s^{-1}$; all tumours, $1.20x10^{-3}mm^2s^{-1}$; p<0.0001), and compared to thymic epithelial tumour group and lymphoma group (p<0.0001) (**Figure 1**). Considering logistic regression models for evaluating the ability of ADC in discrimination of

tumours from LTH, the tumour probability decreased with the increase of ADC (Odds Ratio [OR] *per* 0.01 increase, 0.879; 95%CI, 0.806-0.958; p=0.003). AUROC of ADC in discriminating between groups (LTH versus tumours) was 0.963 (95%CI, 0.865-0.996). The optimal cut-point was identified in ADC value $\leq 1.45 \times 10^{-3} mm^2 s^{-1}$ for tumour diagnosis (Youden Index J = 0.850) (**Figure 1**). Applying this cut-point, for the diagnosis of tumour, sensitivity was 85.0% and specificity was 100%. Overlapped ADC values between groups (LTH versus tumours) were found in the range between 1.61 and $1.77 \times 10^{-3} mm^2 s^{-1}$, although in the tumour group all cases were thymomas (overall, 10 cases with overlapped values, 6 thymomas and 4 LTH). All these cases were low-grade thymomas (A, AB and B1) and non-advanced thymomas (stage I and II) according to the Jeong classification and Masaoka-Koga staging system (**Figure 1**).

About comparison between subgroups of the tumour group, there was no significant difference in ADC values between thymic carcinomas and thymomas, despite the latter had higher mean ADC values ($1.28 \times 10^{-3} mm^2 s^{-1}$ versus $0.95 \times 10^{-3} mm^2 s^{-1}$; p=0.099). Conversely, non-advanced thymomas presented ADC values higher than advanced thymomas, at the limit of statistical significance ($1.42 \times 10^{-3} mm^2 s^{-1}$; $1.13 \times 10^{-3} mm^2 s^{-1}$; p=0.044). At last, Hodgkin lymphomas presented ADC values higher than non-Hodgkin lymphomas ($1.18 \times 10^{-3} mm^2 s^{-1}$; $1.07 \times 10^{-3} mm^2 s^{-1}$), although this difference was not statistically significant (p=0.31).

DCE-MR: Differences in TIC Patterns between Groups and Subgroups

The TIC obtained from each case demonstrated that LTH and mediastinal tumours had low and intermediate perfusion compared to thoracic aorta used as a reference, with LTH-tumour/aorta AUC ratio varying from 5% (in a case of low grade thymoma) to 82% (in a case of thymic carcinoma). Overall, thymic carcinomas showed significantly higher perfusion than lymphomas (AUC_{lesion}/AUC_{aorta}: thymic carcinomas, 63%; lymphomas, 46%; p=0.046), while both showed significantly higher perfusion than thymomas (AUC_{lesion}/AUC_{aorta}: thymomas, 34%; p=0.004; one-way analysis of variance).

The type A TIC pattern (persistent pattern) was found in 20/49 cases (41%), type B (plateau pattern) in 23/49 (47%), type C (wash-out pattern) in 6/49 (12%) (**Figure 4** and **5**, **Table 3**). The type A curve was the prevalent TIC pattern in thymic epithelial tumour group (13/22, 59.1%), particularly in thymoma subgroup (12/19, 63.2%), whereas type B curve was mostly observed in lymphoma group (12/15, 80.0%) and in LTH group (8/9, 88.9%). The type C curve was exclusively found in thymic carcinoma subgroup (2/3, 66.6%) and in 4 out of 9 cases of high grade thymoma (**Table 3**). The type A TIC was significantly more frequent in thymic epithelial tumour group and in thymoma subgroup compared to LTH group and lymphoma group ($p<0.001$). Similarly, the type B TIC was significantly more frequent in LTH group and lymphoma group compared to thymic epithelial tumour group ($p<0.0001$), but not between LTH group and lymphoma group ($p>0.5$).

DCE-MR: Differences in Semi-quantitative Parameters between Groups - Thymomas versus Lymphomas

About discrimination between thymoma and lymphoma, the semi-quantitative analysis of TIC (**Table 3**) showed significant differences for WIR ($p=0.0001$), AUC ($p=0.0014$), and MER ($p<0.0001$) which were higher in lymphomas compared to thymomas (**Figure 2**). The remaining parameters were not significantly different between the two groups. In **table 4**, the logistic regression models, obtained for evaluating the discriminatory abilities of significant semi-quantitative parameters in differentiation between groups, were reported. At univariate analysis, the probability of finding lymphoma increased *per* one unit increase of WIR, AUC, and MER with Odds Ratio (OR) ranging from 1.015 (AUC) to 1.210 (WIR) (OR: lower 95%CI, 1.004 for AUC; higher p of 0.0068 for AUC). About ROC analysis of these parameters, AUROC ranged from 0.828 for AUC (95%CI, 0.660-0.935; sensitivity, 93%; specificity, 58%; cut-point, $157x10^3$) to 0.877 for MER (95%CI , 0.719-0.964; sensitivity, 87%; specificity, 79%; cut-point, 183.7) (**Figure 2**). The comparison between ROC curves showed no significant differences between AUROC of WIR, AUC, and MER (**Figure 2**). The multivariate logistic model, after controlling for patients' age and lesion size, showed that MER was a significant independent predictive parameter in the

differentiation between thymomas and lymphomas (higher p=0.044), while AUC and WIR were not significant parameters (p, 0.89 and 0.36, respectively) (**Table 4**).

DCE-MR: Differences in Semi-quantitative Parameters between Groups - Thymic epithelial tumours versus Lymphomas

About discrimination between thymic ephitelial tumours and lymphomas, the semi-quantitative analysis of TIC (**Table 3**) showed significant differences for WIR (p=0.0003), AUC (p=0.019), and MER (p =0.0006), which were higher in lymphomas compared to thymic epithelial tumours (**Figure 3**). The remaining parameters were not significantly different between the two groups. In **table 4**, the logistic regression models, obtained for evaluating the discriminatory abilities of significant semi-quantitative parameters in differentiation between groups, were reported. At univariate analysis, the probability of finding lymphoma increased *per* one unit increase of WIR, AUC, and MER with Odds Ratio (OR) ranging from 1.008 (AUC) to 1.176 (WIR) (OR: lower 95%CI, 1.0007 for AUC; higher p of 0.003 for AUC). About ROC analysis of these parameters, AUROC ranged from 0.758 for AUC (95%CI, 0.589-0.883; sensitivity, 93%; specificity, 50%; cut-point, $157x10^3$) to 0.809 for MER (95%CI , 0.646-0.919; sensitivity, 87%; specificity, 73%; cut-point, 183.7) (**Figure 3**). The comparison between ROC curves showed a significant higher AUROC of WIR and MER compared to AUC (p=0.013) (**Figure 3**). The multivariate logistic model, after controlling for patients' age and lesion size, showed that WIR and MER were significant independent predictive parameters in the differentiation between thymic epithelial tumours and lymphomas (higher p, 0.022 for MER) (**Table 4**).

DCE-MR: Differences in Parameters between LTH patients and Thymoma patients with overlapped ADC values

In ten cases of overlapped ADC values (6 thymomas, 4 LTH), the most frequent pattern of TIC was type A for thymomas (4/6, 67%; 2/6 cases, type B pattern) and type B for LTH 3/4, 75%, 1/4 cases, type A pattern), but there was no significant difference in ADC values between these cases (p=0.57; chi-square test). Moreover, low perfusion on DCE-MR assessment was found in these cases from

both groups, with no significant differences in AUC compared to aorta (AUC_{lesion}/AUC_{aorta}: thymomas, 26%; LTH, 19%; p=0.40). Overall, these six cases of thymoma were non-advanced (stage I and II) and low-grade (A, AB, B1) thymomas after surgical removal.

Discussion

The present study shows the usefulness of MR in the characterization of lesions located in the anterior mediastinum. In particular, it demonstrates the importance of DW-MR and DCE-MR, through the use of ADC and through the analysis of TIC with calculation of semi-quantitative parameters, in order to optimize the diagnostic efficacy of MR of the anterior mediastinum.

In the last decade, chest MR has been increasingly used for the evaluation of lung, pleura, and mediastinum, thanks to its technological improvement that has allowed the use of faster sequences with better space resolution (Abdel Razek A, 2009; Ackman JB, 2014). Therefore, at present, chest MR is often indicated as a second-level imaging in patients with mediastinal lesions after CT, especially for diagnosis (differentiation between benign conditions and malignant lesions), for local staging (invasion of contiguous structures or detection of pleural and pericardial implants in thymic epithelial tumours), and for detecting distant metastases (lymph node involvement and visceral metastases) (Abdel Razek A, 2012; Ackman JB, 2011; Ackman JB, 2014; Priola AM, 2016; Priola AM 2019).

Quantitative DW-MR, through the measurement of ADC, has proved accurate in the differentiation between malignant lesions (e.g., thymic epithelial tumours and lymphomas) and benign conditions (e.g. ,lymph node involvement in sarcoidosis or tuberculosis; reactive lymphoid hyperplasia; normal or hypertrophic thymus in different clinical conditions) in numerous studies, although overlapped ADC values between benign and malignant conditions have also been reported (Abdel Razek A, 2009; Abdel Razek AAK, 2012; Gümüştaş S, 2013; Priola AM, 2016; Seki S, 2014; Shin KE, 2014). Nevertheless, the diagnostic accuracy of DW-MR in this differentiation has been greater than 80% in previous published studies (Gumustas S, 2011; Abdel Razek AAK, 2012; Seki S, 2014). Our study confirms the diagnostic efficacy of DW-MR in this discrimination, with

significantly higher ADC values in LTH compared to tumour group and diagnostic accuracy greater than 90%. However, similarly to other studies, in our cohort the DW-MR was ineffective in the distinction of different mediastinal tumours, in particular in differentiating thymomas from lymphomas, which represent the most frequent tumours detected in the anterior mediastinum (Nishino M, 2006; Priola AM, 2006; Seki S, 2014; Yabuuchi H, 2015).

Pre-operative differentiation between lymphomas and other mediastinal tumours, based on diagnostic imaging, is useful since treatments are different in these cases (Yabuuchi H, 2015). As an example, a thoracotomic approach for surgical biopsy in order to obtain the correct diagnosis could be avoided in patients with lymphoma, who only need chemotherapy, considering that currently thoracic surgeons avoid preoperative biopsy of an anterior mediastinal lesion which can be easily removed based on CT and MR imaging because of the absence of clear infiltration of the adjacent structures or of distant metastases, findings that are highly suggestive for thymoma (Girard N, 2015; Ruffini E, 2011). In these cases, interpretative errors could occur, especially in the differential diagnosis with primary mediastinal lymphoma (i.e., lymphoma with the exclusive involvement of the anterior mediastinal compartment), which represents 15% of all mediastinal lymphomas, in asymptomatic patients (i.e., in the absence of specific B symptoms based on Ann-Arbor classification for lymphoma or in the absence of signs and symptoms suggestive for generalized myasthenia gravis for thymoma) (Priola AM, 2006). Furthermore, the characterization of mediastinal tumours based on diagnostic imaging would be useful for the correct planning of treatments, since some conditions require neo-adjuvant therapy before surgical resection, such as germ cell tumours or advanced thymomas (stage III and IV, Masaoka-Koga staging system) conversely to non-advanced thymomas (stage I-II) (Girard E, 2015; Priola AM, 2014; Yabuuchi H, 2015). About this topic, our study has demonstrated the efficacy of DCE-MR, by evaluating TIC patterns and by using some semi-quantitative parameters obtained from TIC, in the differentiation between thymomas and thymic epithelial tumours from lymphomas, that reflects the different perfusion over time of these tumours.

To date, only two studies have investigated the usefulness of DCE-MR in characterizing mediastinal lesions. In 2002, Sakai and collaborators (Sakai S, 2002) assessed the ability of DCE-MR in the distinction between thymomas and non-thymomatous lesions (that include thymic carcinomas, thymic carcinoids, squamous and small cell carcinomas, undifferentiated carcinomas, germ cells, and lymphomas) by evaluating TTP, as the unique semi-quantitative parameter of TIC, and TIC pattern. In their study, thymomas presented an early TTP (mean value, 1.5 min) compared to non-thymomas (mean value, 3.2 min). In addition, non-advanced thymomas were characterized by a significantly lower TTP than advanced thymomas (1.3 versus 2.5 min, respectively). Overall, the authors reported sensitivity and specificity of 79% and 84% in this discrimination, considering, as cut-point, a TTP value of less than 2 minutes for the diagnosis of thymoma and greater than 2.5 minutes for the diagnosis of non-thymoma. Conversely, in our study, TTP did not demonstrate significant differences between thymomas and other tumours (including thymic carcinomas, lymphomas, and germ cell tumours), although the mean value of TTP was lower in thymomas (199 seconds) compared to other tumours (210 and 233 seconds for thymic carcinomas and lymphomas, respectively). In addition, TTP of LTH was not significantly different from that of tumour group. This finding supports the ineffectiveness of semi-quantitative assessment of DCE-MR based solely on the evaluation of TTP. More recently, Yabuuchi and collaborators (Yabuuchi H, 2015) assessed the effectiveness of the association of DW-MR, DCE-MR, and FDG-PET/CT in the characterization of solid anterior mediastinal tumours. About DCE-MR, the authors defined three types of TIC, based on TTP (arbitrarily referred to 120 seconds) and WOR (arbitrarily referred to 30% in comparison with PE), which were divided as follows: "persistent" pattern (TTP>120 sec), "plateau" pattern (TTP≤120 sec; WOR≤30%), and "wash-out" pattern (TTP≤120 sec; WOR>30%). In this study, none of the 19 lymphoma patients had a wash-out patterns. The persistent pattern was infrequent both in the lymphoma group (4/19, 21%) and in the thymic epithelial tumour group (1/71, 1.4%; a single case of thymic carcinoma). The plateau pattern was frequent in both groups (lymphoma: 15/19, 79%; thymic epithelial tumours: 32/71, 45%). Therefore, by considering this

study, it can be concluded that the finding of wash-out pattern excludes the diagnosis of lymphoma, while the finding of persistent pattern most likely excludes the diagnosis of thymic epithelial tumour. However, in the study, a large proportion of lesions (47/71, 66%) with plateau pattern cannot be characterized. Furthermore, the discrimination of TIC pattern based on TTP (cut-point, 120 seconds) is questionable in the definition of a curve with a "plateau" which peak has a signal intensity slightly higher compared to the other time-points of TIC. On the contrary, in our study, different results were obtained in the evaluation of TIC pattern: in particular, we did not find cases of significant wash-out in all cases, except for the majority of thymic carcinomas and some thymomas (all high grade thymomas). For all other cases, WOR was constantly lower than 30%. Persistent pattern was found mainly in the the thymic epithelial tumour group (13/20, 65%), whereas plateau pattern was found mainly in the lymphoma group (12/23, 52%). Thus, in our study and conversely to quantitative DW-MR, the evaluation of TIC pattern of DCE-MR was found effective in the distinction between lymphomas and thymomas.

Neither of the two studies on DCE-MR of the anterior mediastinum evaluated the usefulness of semi-quantitative parameters obtained from TIC for diagnosing different abnormalities of the anterior mediastinum, although they were found reliable in previously published papers on the evaluation of tumours in different compartments (Coolen J, 2014; Coolen J, 2015 ; Liu HL, 2018; Manganaro L, 2018). As an example, Coolen and collaborators (Coolen J, 2015) have demonstrated the effectiveness of DCE-MR, in addition to DW-MR, in increasing the sensitivity of MR in differentiating pleural mesothelioma from benign pleural conditions. In addition, the same study group demonstrated the usefulness of DCE-MR in differentiating benign and malignant solitary pulmonary nodules, showing an increase in specificity of DCE-MR in association with DW-MR (Coolen J, 2014). However, similarly to the studies of Sakai et al. and Yabuuchi et al., these last studies are based on morphological analysis of TIC obtained by considering few semi-quantitative parameters. A more extensive evaluation of semi-quantitative parameters derived from TIC has demonstrated their effectiveness in discriminating between benign and malignant lesions of breast

and testicle (Liu H-L, 2018; Manganaro L, 2018). In both compartments, different semi-quantitative parameters were found to be reliable in this discrimination, with better diagnostic performance of SI_{slope} for breast and AUC for testis (AUROC, 0.756 and 0.890, respectively) (Liu HL, 2018; Manganaro L, 2018). In our study, the analysis of same semi-quantitative parameters obtained from TIC was useful in discriminating between lymphomas and thymomas or thymic epithelial tumours. Most of mediastinal lesions had low perfusion compared to aorta. Moreover, WIR and MER were found to be effective and significant independent predictive parameters in this discrimination. The morphological analysis of TIC based on TTP and WOR has proved useful in this distinction, although TTP and WOR parameters were not significantly different between groups. Therefore, the use of semi-quantitative parameters of TIC should be performed in indeterminate cases, as an integration of TIC pattern analysis.

Considering cases of LTH and thymoma with overlapped ADC values at DW-MR, our study demonstrated that TIC pattern of DCE-MR can help in this discrimination, because persistent pattern is more frequent in low-grade and non-invasive thymomas, whereas plateau pattern is more appreciable in LTH. However, no significant differences between these cases were found presumably due to the small study cohort. Nevertheless, in these cases, morphological evaluation is mandatory, since round or oval morphology is typical of thymomas while triangular or trapezoidal morphology is usually seen in LTH, although morphological overlaps in both conditions have been reported (Ackman JB, 2015; Inaoka T, 2015; Priola AM, 2015; Araki T, 2014).

The present study has some limitations. First, although the cohort included a fair number of cases in relation with the anatomical compartment investigated, the sample size of LTH was limited to a small number. Indeed, in LTH, only cases of non-suppressing hyperplasia at chemical-shift MR (because of the poor fatty tissue content) were selected, a condition rarely reported for the thymus (normal thymus, LTH, rebound thymic hyperplasia) in previous studies, mostly in adolescents and young adults (Takahashi K, 2003; Inaoka T, 2005; Ackman JB, 2012; Priola AM, 2015; Priola AM, 2018; Phung T, 2018). Second, a selection bias cannot be excluded because only subjects with

mediastinal lesions with available histological diagnosis, which was considered the reference standard, were enrolled. Third, specific pharmacokinetic parameters of DCE-MR (e.g., K_{trans} [volume transfer constant], K_{ep} [rate constant], and V_e [extravascular extracellular space volume fraction]) were not evaluated. These parameters, which were found useful in previous studies evaluating tumours of different compartments, could improve diagnostic accuracy of MR in characterizing anterior mediastinal tumours. Finally, although the proposed cut-off values of ADC from DW-MR and semi-quantitative parameters of TIC from DCE-MR showed effective discriminatory abilities between different conditions of the anterior mediastinum (especially, for DCE-MR, between thymomas or thymic epithelial tumors and lymphomas, which represent most of the anterior mediastinal tumours), these results were derived from the data analyzed and need to be validated in independent samples of patients before recommending their use in clinical practice.

In conclusion, in addition to DW-MR, DCE-MR is useful in characterizing anterior mediastinal findings. In particular, DW-MR through ADC measurement has proven effective in the distinction between tumours and LTH, although it may have limits in differentiating LTH from non-advanced thymoma; however, it is not reliable in the differentiation between different tumours (i.e., thymoma or thymic epithelial tumours versus lymphomas). The analysis of TIC pattern and of semi-quantitative parameters obtained by using DCE-MR is conversely effective in the characterization of different mediastinal tumours, especially in the differentiation of thymomas and thymic epithelial tumours from lymphomas, with significant discriminatory ability for MER and WIR. Moreover, DCE-MR may be useful in the discrimination between non-invasive thymomas and LTH, where overlapped ADC values can be found, although our data are to be confirmed in further studies with larger sample size.

References

- Abdel Razek A, Elmorsy A, Elshafey et al. Assessment of mediastinal tumors with diffusion weighted single shot echo planar MR imaging. J Magn Reson Imaging 2009;30:535-40.
- Abdel Razek AAK. Diffusion magnetic resonance imaging of chest tumors. Cancer Imaging 2012;12:452-63.
- Abdel Razek A, Soliman N, Elashery R. Apparent diffusion coefficient values of mediastinal masses in children. Eur J Radiol 2012;81:1311-4.
- Abdel Razek AA, Khairy M, Nada N. Diffusion-weighted MR imaging in thymic epithelial tumors: correlation with World Health Organization classification and clinical staging. Radiology 2015;273:268-75.
- Ackman JB, Wu CC. MRI of the thymus. AJR Am J Roentgenol 2011;197:W15-20.
- Ackman JB, Mino-Kenudson M, Morse CR. Nonsuppressing normal thymus on chemical shift magnetic resonance imaging in a young woman. J Thoracic Imaging 2012;27:196-8.
- Ackman JB. A practical guide to nonvascular thoracic magnetic resonance imaging. J Thorac Imaging 2014;29:17-29.
- Ackman JB, Verzosa S, Kovach AE, et al. High rate of unnecessary thymectomy and its cause. Can computed tomography distinguish thymoma, lymphoma, thymic hyperplasia, and thymic cysts? Eur J Radiol 2015;84:524-33.
- Araki T, Sholl LM, Gerbaudo VH, et al. Imaging characteristics of pathologically proven thymic hyperplasia: identifying features that can differentiate true from lymphoid hyperplasia. AJR 2014; 202:471-8.
- Coolen J, De Keyzer F, Nafteux P, et al. Malignant pleural disease: diagnosis by using diffusion-weighted and dynamic contrast-enhanced MR imaging—initial experience. Radiology 2012;263:884-92.

- Coolen J, Vansteenkiste J, De Keyzer F, et al. Characterisation of solitary pulmonary lesions combining visual perfusion and quantitative diffusion MR imaging. Eur Radiol 2014;24:531-41.
- Coolen J, De Keyzer F, Nafteux P, et al. Malignant pleural meosthelioma: visual assessment by using pleural pointillism at diffusion-weighted MR imaging. Radiology 2015;274:576-84.
- Girard N, Ruffini E, Marx A, et al. Thymic epithelial tumours: ESMO clinical practice guidelines for diagnosis, treatment and follow-up. Ann Oncol 2015;26:v40-v55.
- Gümüştaş S, Inan N, Sarisoy HT, et al. Malignant versus benign mediastinal lesions: quantitative assessment with diffusion weighted MR imaging. Eur Radiol 2011;21:2255-60.
- Gümüştaş S, Inan N, Akansel G, et al. Differentiation of lymphoma versus sarcoidosis in the setting of mediastinal-hilar lymphadenopathy: assessment with diffusion-weighted MR imaging. Sarcoidosis Vasc Diffuse Lung Dis 2013;30:52-9.
- Inaoka T, Takahashi K, Iwata K, et al. Evaluation of normal fatty replacement of the thymus with chemical-shift MR imaging for identification of the normal thymus. J Magn Reson Imaging 2005;22:341-6.
- Inaoka T, Takahashi K, Mineta M, et al. Thymic hyperplasia and thymus gland tumors: differentiation with chemical shift MR imaging. Radiology 2007;243:869-76.
- Kono M, Adachi S, Kusumoto M, et al. Clinical utility of Gd-DTPA-enhanced magnetic resonance imaging in lung cancer. J Thorac Imaging 1993;8:18-26.
- Liu H-L, Zong M, Wei H, et al. Differentiation between malignant and benign breast masses: combination of semi-quantitative analysis on DCE-MRI and histogram analysis of ADC maps. Clin Radiol 2018; *In Press*.
- Manganaro L, Saldari M, Pozza C, et al. Dynamic contrast-enhanced and diffusion-weighted MR imaging in the characterisation of small, non-palpable solid testicular tumours. Eur Radiol 2018;28:554-564.

- Nishino M, Ashiku SK, Kocher ON, Thurer RL, Boiselle PM, Hatabu H. The thymus: a comprehensive review. Radiographics 2006;26:335-48.
- Padhani AR, Guoying L, Mu-Koh D, et al. Diffusion-weighted magnetic resonance imaging as a cancer biomarker: consensus and recommendations. Neoplasia 2009;11:102-25.
- Phung T, Nguyen T, Tran D, et al. A thymic hyperplasia case without suppressing on chemical shift magnetic resonance imaging. Case Rep Radiol 2018; *In Press.*
- Priola AM, Priola SM, Cardinale L, Cataldi A, Fava C. The anterior mediastinum: diseases. Radiol Med 2006;111:312-42.
- Priola AM, Priola SM. Imaging of thymus in myasthenia gravis: from thymic hyperplasia to thymic tumor. Clin Radiol 2014;69:e230-45.
- Priola AM, Priola SM, Ciccone G, et al. Differentiation of rebound and lymphoid thymic hyperplasia from anterior mediastinal tumors with dual-echo chemical-shift magnetic resonance imaging in adulthood: reliability of the chemical-shift ratio and signal-intensity index. Radiology 2015;274:238-49.
- Priola AM, Priola SM, Giraudo MT, et al. Chemical-shift and diffusion-weighted magnetic resonance imaging of thymus in myasthenia gravis: usefulness of quantitative assessment. Invest Radiol 2015;50:228-38.
- Priola AM, Priola SM, Gned D et al. Diffusion-weighted magnetic resonance quantitative imaging to diagnose benign conditions from malignancies of the anterior mediastinum: improvement of diagnostic accuracy by comparing perfusion-free to perfusion-sensitive measurements of the apparent diffusion coefficient. J Magn Reson Imaging 2016;44:758-769.
- Priola AM, Gned D, Veltri A, et al. Chemical shift and diffusion-weighted magnetic resonance imaging of the anterior mediastinum in oncology: current clinical applications in qualitative and quantitative assessment. Crit Rev Oncol Hematol 2016;98:335-57.

- Priola AM, Priola SM, Gned D, et al. Nonsuppressing normal thymus on chemical-shift MR imaging and anterior mediastinal lymphoma: differentiation with diffusion-weighted MR imaging by using the apparent diffusion coefficient. Eur Radiol 2018;28:1427-37.
- Priola AM, Gned D, Veltri A, et al. Case 261: Thymoma embedded in thymus with pleural implant in myasthenia gravis Lambert-Eaton Overlap Syndrome. Radiology 2019;290-264-9.
- Raptis CA, Ratkowski KL, Broncano J, et al. Mediastinal and pleural MR imaging: Practical approach for daily practice. Radiographics 2018;38:37-55.
- Ruffini E, Van Raemdonck D, Detterbeck F, et al. Management of thymic tumors. A survey of current practice among members of the european society of thoracic surgeons. J Thorac Oncol 2011;6:614-23.
- Sakai S, Murayama S, Soeda H, et al. Differential diagnosis between thymoma and non-thymoma by dynamic MR imaging. Acta Radiol 2002;43:262-8.
- Seki S, Koyama H, Ohno Y, et al. Diffusion-weighted MR imaging vs. multi-detector row-CT: direct comparison of capability for assessment of management needs for anterior mediastinal solitary tumors. Eur J Radiol 2014;83:835-42.
- Shin KE, Yi CA, Kim TS, Lee HY, Choi YS, Kim HK, et al. Diffusion-weighted MRI for distinguishing non-neoplastic cysts from solid masses in the mediastinum: problem-solving in mediastinal masses of indeterminate internal characteristics on CT. Eur Radiol 2014;24:677-84.
- Schaefer JF, Vollmar J, Schick F et al. Solitary pulmonary nodules: dynamic contrast-enhanced MR imaging-perfusion differences in malignant and benign lesions. Radiology 2004; 232:544-53.
- Takahashi K, Inaoka T, Murukami N, et al. Characterization of the normal and hyperplastic thymus by chemical-shift MR imaging. AJR Am J Roentgenol 2003;180:1265-9.

- Yabuuchi H, Matsuo Y, Abe K, et al. Anterior mediastinal solid tumours in adults: characterisation using dynamic contrast-enhanced MRI, diffusion-weighted MRI, and FDG-PET/CT. Clin Radiol 2015;70:1289-98.

Tables

Table 1

Dynamic Contrast-Enhanced and diffusion-Weighted MR Imaging Pulse Sequence Parameters[§]

Parameter	T1-weighted three-dimensional gradient-echo dynamic contrast-enhanced imaging	T2-weighted single-shot spin-echo echo-planar diffusion-weighted imaging
Acquisition plane	Axial	Axial
Field of view (mm)	375	340
Matrix	288 x 288	224 x 116
Parallel acquisition technique	Sensitivity encoding	Sensitivity encoding
Sensitivity encoding reduction factor	2.59	2
No. of sections	22	32
Section thickness (mm)	5	5
Intersection gap (mm)	0	0
Repetition time (ms)	5.64	2500-3500*
Echo time (ms)	4	62
Flip angle (degrees)	15	90
Phase-encoding direction	Anterior-to-posterior	Anterior-to-posterior
No. of signals acquired	1	4
Fat suppression	Dixon	Spectral pre-saturation attenuated by inversion recovery
No. of images per section	40	4
Bandwidth (Hz/pixel)	723	2615
b-values (s/mm^2)	--	0, 150, 500, 800
Respiratory control	Breath hold	Trigger
Acquisition time (min:s)	00:20	02:05

[§] The MR protocol also included T2-weighted single-shot turbo spin-echo imaging without and with fat suppression (repetition time/Echo time, 386/100 and 415/80 ms, respectively; matrix, 224 x 224; section thickness/intersection gap, 5/0 mm) and T1-weighted dual gradient-echo chemical-shift imaging (repetition time, 154 ms; echo time in-phase/opposed-phase, 4.6/2.3 ms; matrix, 224 x 224; section thickness/intersection gap, 5/0 mm).
* In respiratory-triggered sequences, repetition time is based on the duration of the respiratory cycle.

Table 2

Demographic Characteristic of the Enrolled Population

Group and Subgroup	No. of Patients	Male/Female Ratio	Age (y)*	Size (mm)*[ǂ]
Thymic epithelial tumours	22	13/9	59.7 ± 14.2 (28-82)	62.8 ± 23.7 (21.3-107)
Thymoma	19	11/8	58.7 ± 14.7 (28-82)	62.4 ± 24.4 (21.3-107)
Thymic carcinoma	3	2/1	66.3 ± 10.1 (60-78)	65.4 ± 23.5 (38.3-79.3)
Lymphoma	15	8/7	37.4 ± 21.3 (15-78)	83.4 ± 16.9 (57.7-118)
Hodgkin lymphoma	11	5/6	40.5 ± 23.6 (17-78)	79.2 ± 16.3 (57.7-118)
Non-Hodgkin lymphoma	4	3/1	28.8 ± 11.5 (15-42)	95.0 ± 14.6 (82.3-116)
Thymus[‖]	9	1/8	32.3 ± 17.5 (17-61)	43.4 ± 14.7 (22-66.7)
Lymphoid hyperplasia				
Lymph node metastasis	2	0/2	63.0 ± 2.8 (61-65)	45.8 ± 18.1 (33-58.7)
Germ cell tumour	1	0/1	30	118.7

* Data are mean ± standard deviation with range in parenthesis because of normal distribution of data.
[ǂ] Size is measured on the axial image containing the largest portion of the tissue.
[‖] All patients underwent extended thymectomy for generalized myasthenia gravis.

Table 3

ADC of DW-MR, TIC Pattern and Semi-quantitative TIC Parameters of DCE-MR of Groups and Subgroups

Group and Subgroup	No. of Patients	ADC ($x10^{-3}mm^2s^{-1}$)*	TIC pattern			Semi-quantitative analysis of TIC*									
			A	B	C	TTP	WIR	WOR	AUC$x10^3$	MER	PE	SI_{slope}	ESER	IE_p	SE_p
Thymic epithelial tumours	22	1.24 ± 0.33 (0.73-1.77)	13	3	6	204	17.4	5.1	181	158.4	388.3	1.4	244.5	71.6	42.5
Thymoma	19	1.28 ± 0.32 (0.77-1.77)	12 (7L-5H)	3 (3L)	4 (4H)	206	16.1	5.1	157	145.0	343.7	1.3	215.0	63.5	41.2
Thymic carcinoma	3	0.95 ± 0.25 (0.73-1.22)	1	0	2	190	25.6	4.9	338	243.4	671.2	1.6	431.2	123.1	50.5
Lymphoma	15	1.15 ± 0.17 (0.81-1.42)	3	12	0	220	28.8	7.8	265	222.0	424.1	1.6	208.8	93.0	45.6
Hodgkin lymphoma	11	1.18 ± 0.17 (0.81-1.42)	2	9	0	193	30.7	8.1	288	225.5	447.6	1.7	218.3	101.7	46.8
Non-Hodgkin lymphoma	4	1.07 ± 0.19 (0.90-1.33)	1	3	0	292	23.6	7.2	204	212.6	360.4	1.4	182.5	69.1	42.0
Lymphoid thymic hyperplasia	9	1.86 ± 0.19 (1.61-2.07)	1	8	0	227	15.4	7.3	138	141.9	427.7	0.8	214.3	62.8	31.5
Lymph node metastasis	2	1.12 ± 0.03 (1.09-1.14)	2	0	0	75	34.9	4.9	321	309	528.6	1.9	285.3	263.6	28.7
Germ cell tumour	1	1.44	1	0	0	390	28.5	0	259	457.1	956	2.9	188.5	165.2	87.7

ADC, apparent diffusion coefficient; TIC, time-signal intensity curve; TTP, time to peak; WIR, wash in ratio; WOR, wash out ratio; AUC, area under the curve; MER, maximum enhancement ratio; PE, peak enhancement; SI_{slope}, signal intensity slope; ESER, early signal enhancement ratio; IE_p, initial percentage of enhancement; SE_p, second enhancement percentage.

TIC pattern: A, Persistent; B, Plateau; C, Wash out.

L = Low grade thymoma ($WHO_{Jeong\ classification}$: A, AB, B1); H = High grade thymoma ($WHO_{Jeong\ classification}$: B2, B3)

* Data are mean ± standard deviation, with range in parenthesis.

Table 4

Logistic regression models for evaluating discrimination abilities between lymphomas and thymomas or thymic epithelial tumors of different semi-quantitative TIC parameters

Parameter	Univariate model		Multivariate model‡	
	Odds Ratio*	*p*	Odds Ratio*	*p*
Thymoma vs. lymphoma				
WIR per 1.0 increase	1.210 (1.062-1.379)	0.0041	1.162 (0.837-1.613)	0.3688
AUC per 1 x 10^3 increase	1.015 (1.004-1.026)	0.0068	1.002 (0.968-1.037)	0.8919
MER per 1.0 increase	1.039 (1.011-1.067)	0.0060	1.049 (1.001-1.090)	0.0445
Thymic epithelial tumour vs. lymphoma				
WIR per 1.0 increase	1.176 (1.051-1.315)	0.0046	1.141 (1.033-1.376)	0.0097
AUC per 1 x 10^3 increase	1.008 (1.001-1.165)	0.0337	0.982 (0.964-1.001)	0.0717
MER per 1.0 increase	1.022 (1.005-1.038)	0.0088	1.030 (1.004-1.058)	0.0227

TIC, time-signal intensity curve; WIR, wash in ratio; AUC, area under the curve; MER, maximum enhancement ratio.

‡ Multivariate model was obtained after controlling for age and size.

* Numbers in parentheses are 95% confidence intervals.

Figures and figure captions

Figure 1:

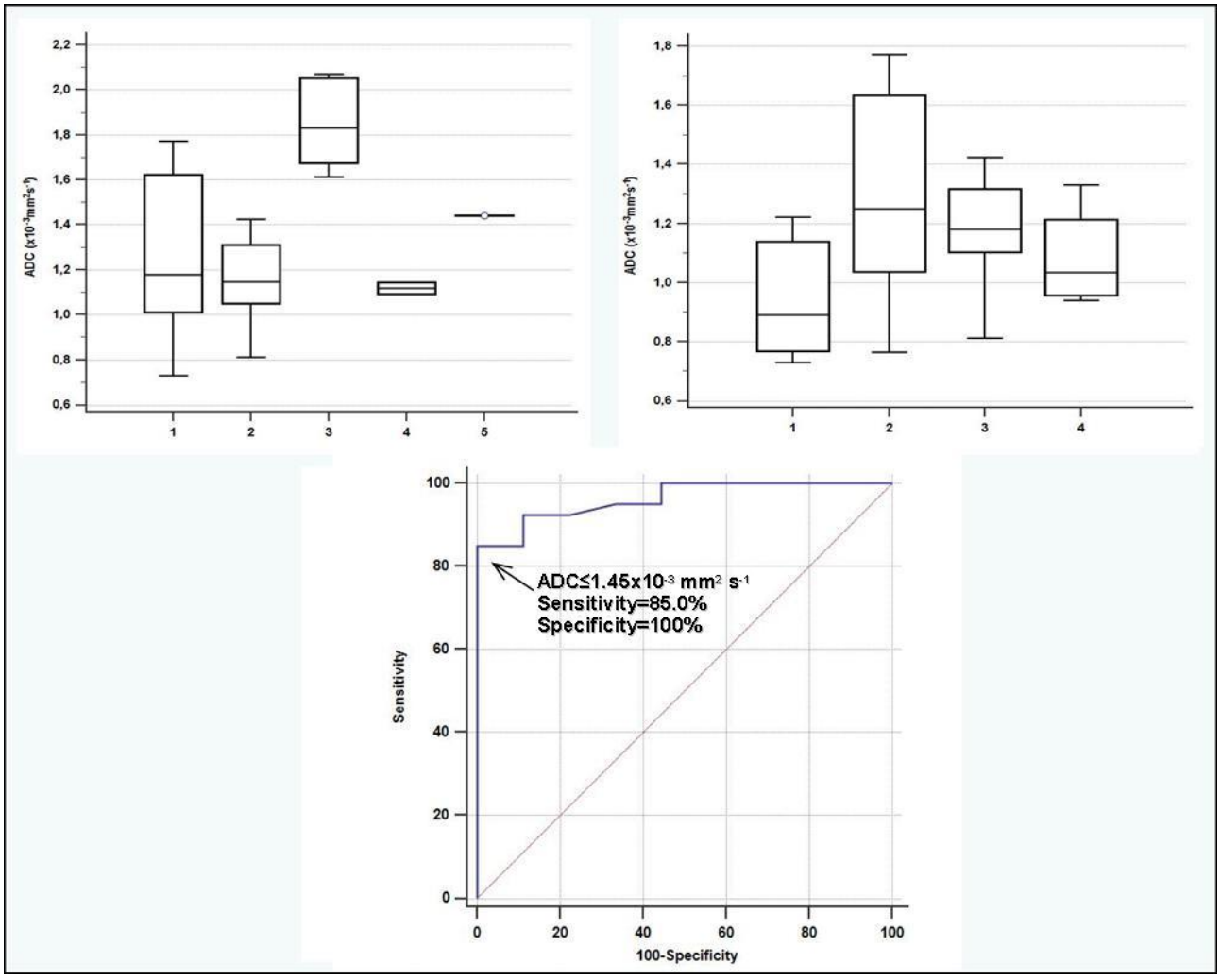

(Upper panels) Box-and-whisker plots show the ADC values for **(left panel)** all groups and **(right panel)** subgroups of thymic epithelial tumour group and lymphoma group. ADC values of each case are marked by red dots as individual data points. The line inside each box represents the median value (50th percentile). Note that overlap in ADC values is exclusively seen between lymphoid thymic hyperplasia group and thymic epithelial tumour group (all cases of overlap in the thymic epithelial tumour group classified, after surgical resection, as Masaoka-Koga stage I or II thymomas, and as WHO type A, AB or B1 thymomas). Groups and subgroups include patients with thymic epithelial tumour (left panel, 1), lymphoma (left panel, 2), lymphoid thymic hyperplasia associated with generalized myasthenia gravis (left panel, 3), lymph node metastases from breast

cancer (left panel, 4), germ cell tumour (left panel, 5), thymic carcinoma (right panel, 1), thymoma (right panel, 2), Hodgkin's lymphoma (right panel, 3), non-Hodgkin's lymphoma (right panel, 4). **(Lower panel)** Receiver operating characteristic curve of ADC indicates the sensitivities and specificities at variable ADC values in the differentiation between anterior mediastinal tumours and LTH. The optimal cut-off value for this discrimination is highlighted with the relative values of sensitivity and specificity.

Figure 2:

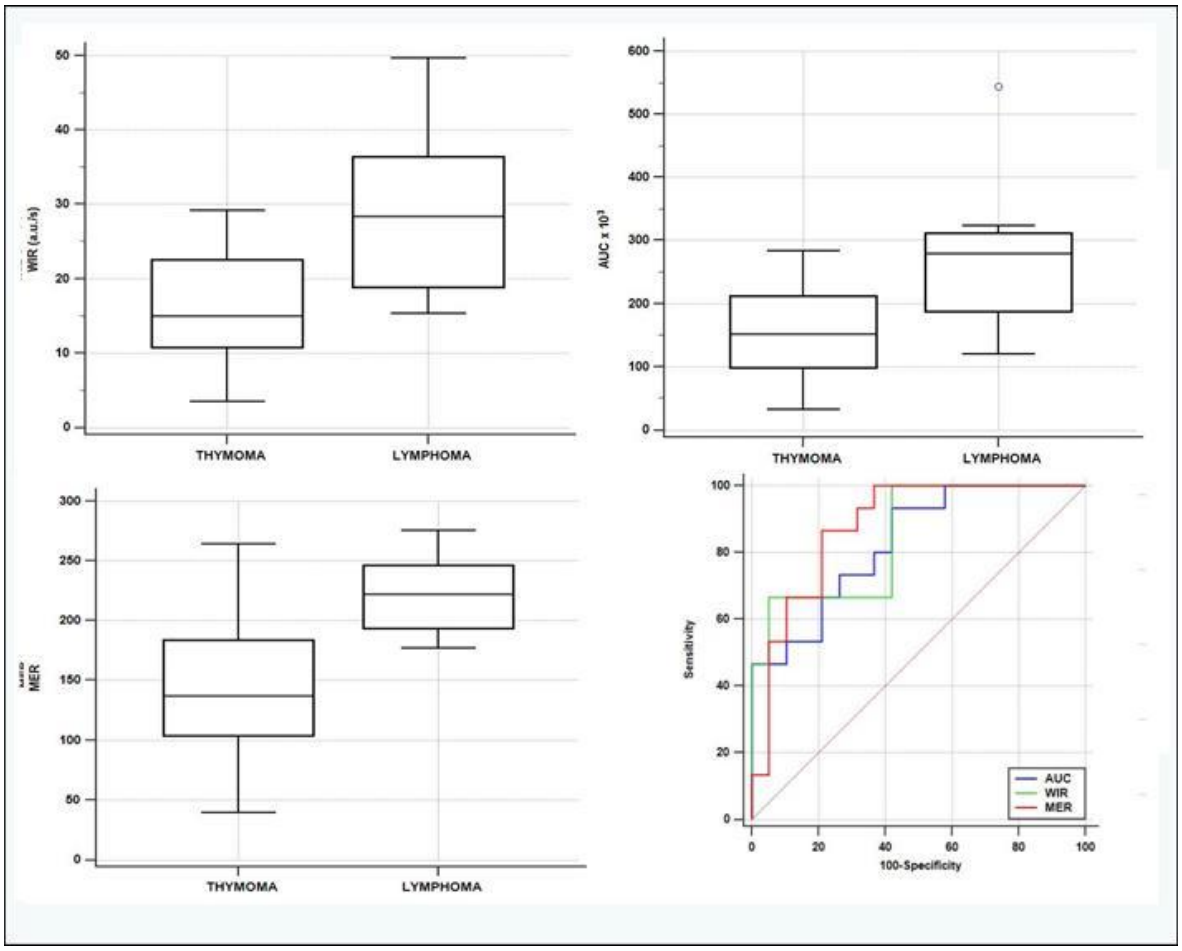

(Left and central panels) Box-and-whisker plots show significant semi-quantitative parameters obtained from the time-signal intensity curve of DCE-MR imaging in discriminating between thymoma group and lymphoma group. **(Right panel)** Graphs show comparison of receiver operating characteristic curves for differentiating thymoma group from lymphoma group by using WIR, AUC, and MER.

Figure 3:

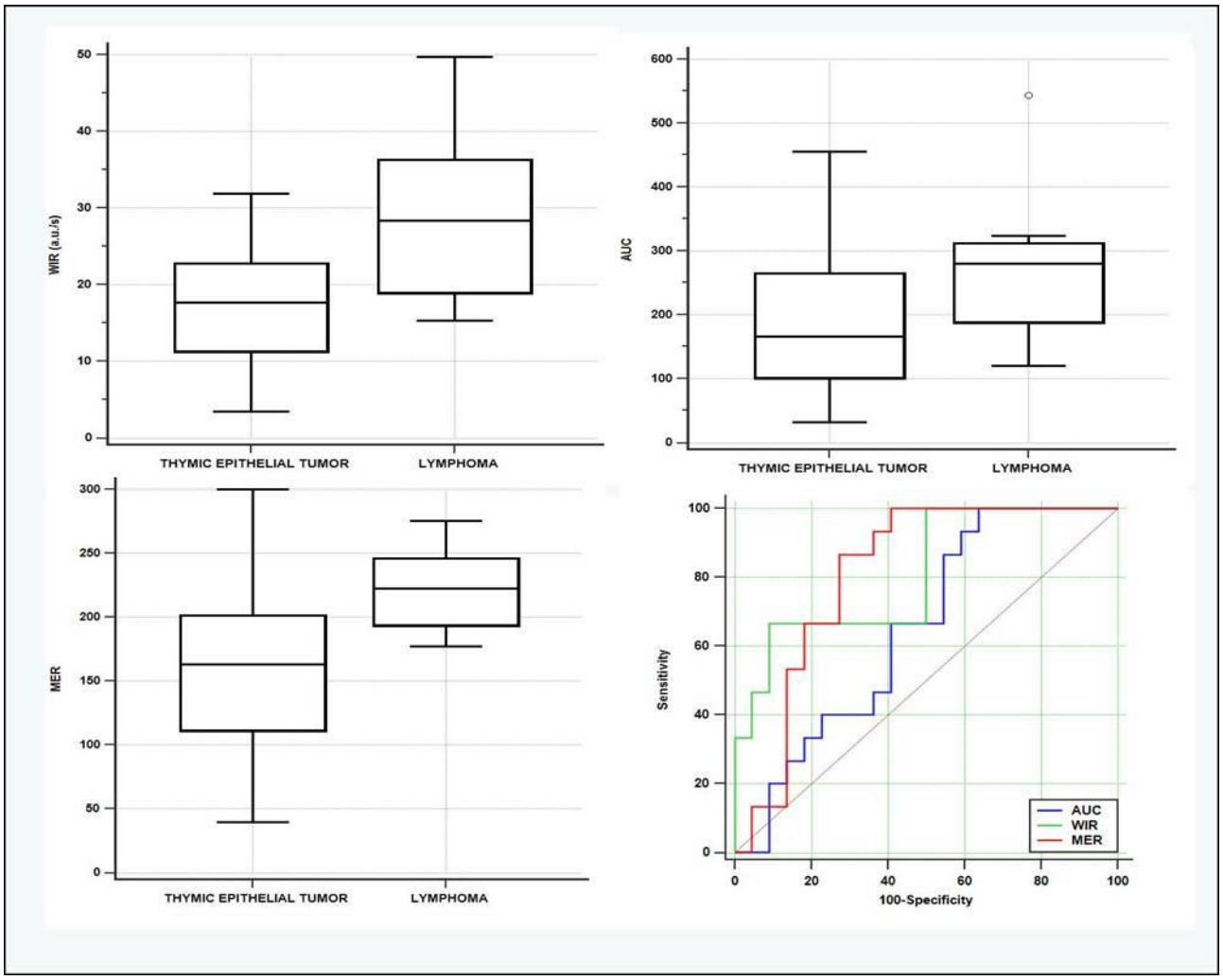

(Upper panels and lower left panel) Box-and-whisker plots show significant semi-quantitative parameters obtained from the time-signal intensity curve of DCE-MR imaging in discriminating between thymic epithelial tumours group and lymphoma group. **(Lower right panel)** Graphs show comparison of receiver operating characteristic curves for differentiating thymic epithelial tumours group from lymphoma group by using WIR, AUC, and MER.

Figure 4:

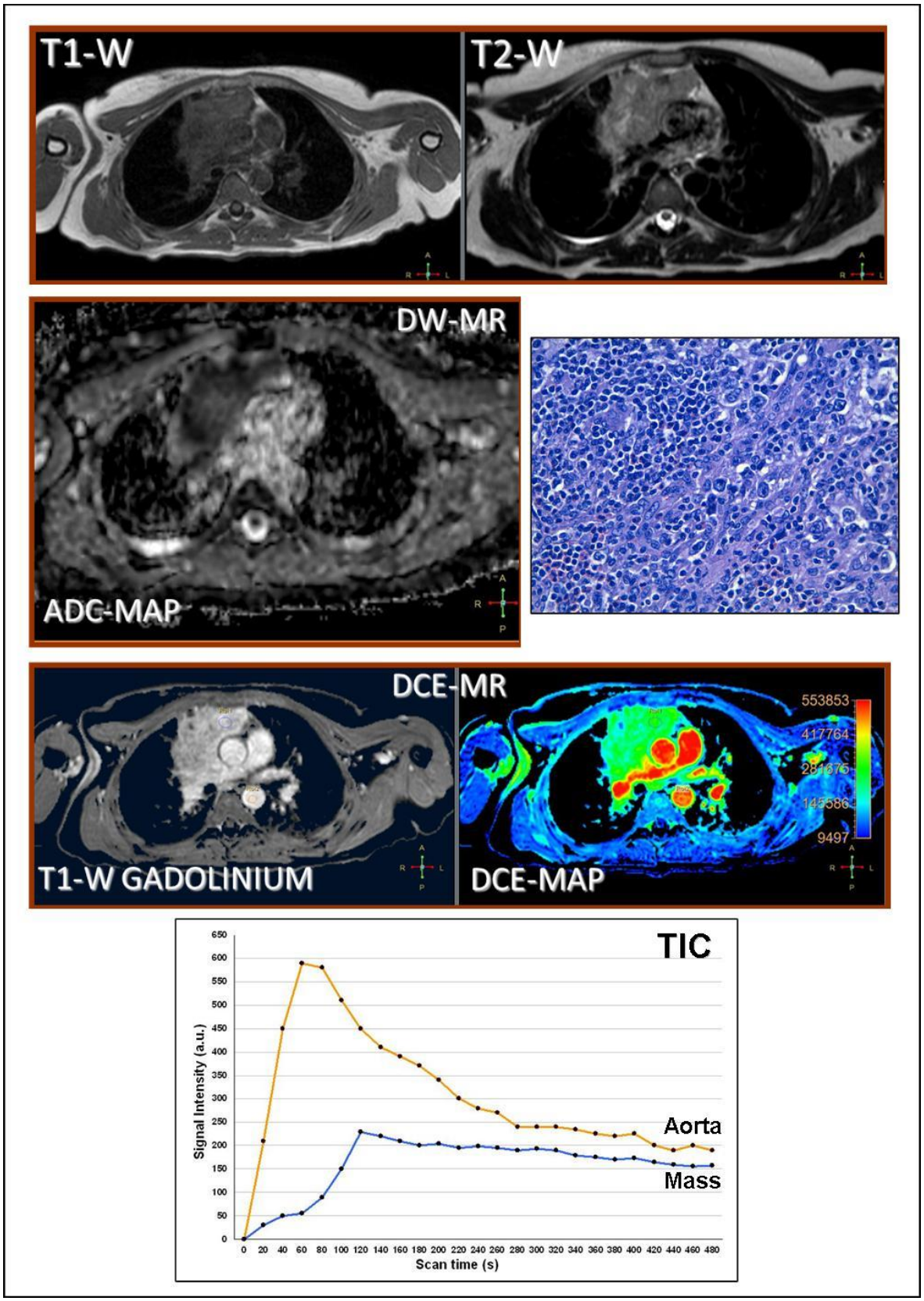

Primary mediastinal Hodgkin's lymphoma (scleronodular variant) in a 37-year-old woman.

Transverse T1-weighted (**T1-W**) and T2-weighted with no fat suppression (**T2-W**) magnetic resonance images show a huge mass in the anterior mediastinum with soft tissue attenuation, inhomogeneous signal intensity, and mild right pleural effusion. The signal intensity is similar than that of muscles in T1-W imaging and higher compared to muscles in T2-W imaging.

Apparent diffusion coefficient map (**ADC-map)** of diffusion-weighted magnetic resonance imaging shows a low-signal intensity lesion for restricted diffusion to the water molecules movement, with ADC of $0.81x10^{-3}mm^2/s$.

Dynamic contrast-enhanced magnetic resonance (**DCE-MR**) shows a bulky mass in the anterior mediastinum, with diffuse low vascularisation, an intermediate ratio compared to aorta, and a plateau pattern of time-signal intensity curve (time to peak of 120s, wash out ratio less than 5%).

Photomicrograph of a representative histological section of Hodgkin's lymphoma, obtained after core biopsy, shows a polymorphic high cellular proliferation within the nodules, with small and large lymphocytes, plasma cells, eosinophils and histiocytes. Scattered lacunar cells (Reed-Sternberg cell variant) are detected in small clusters or isolated. No fat cells are appreciable (Hematoxylin and eosin stain; original magnification, x400).

Figure 5:

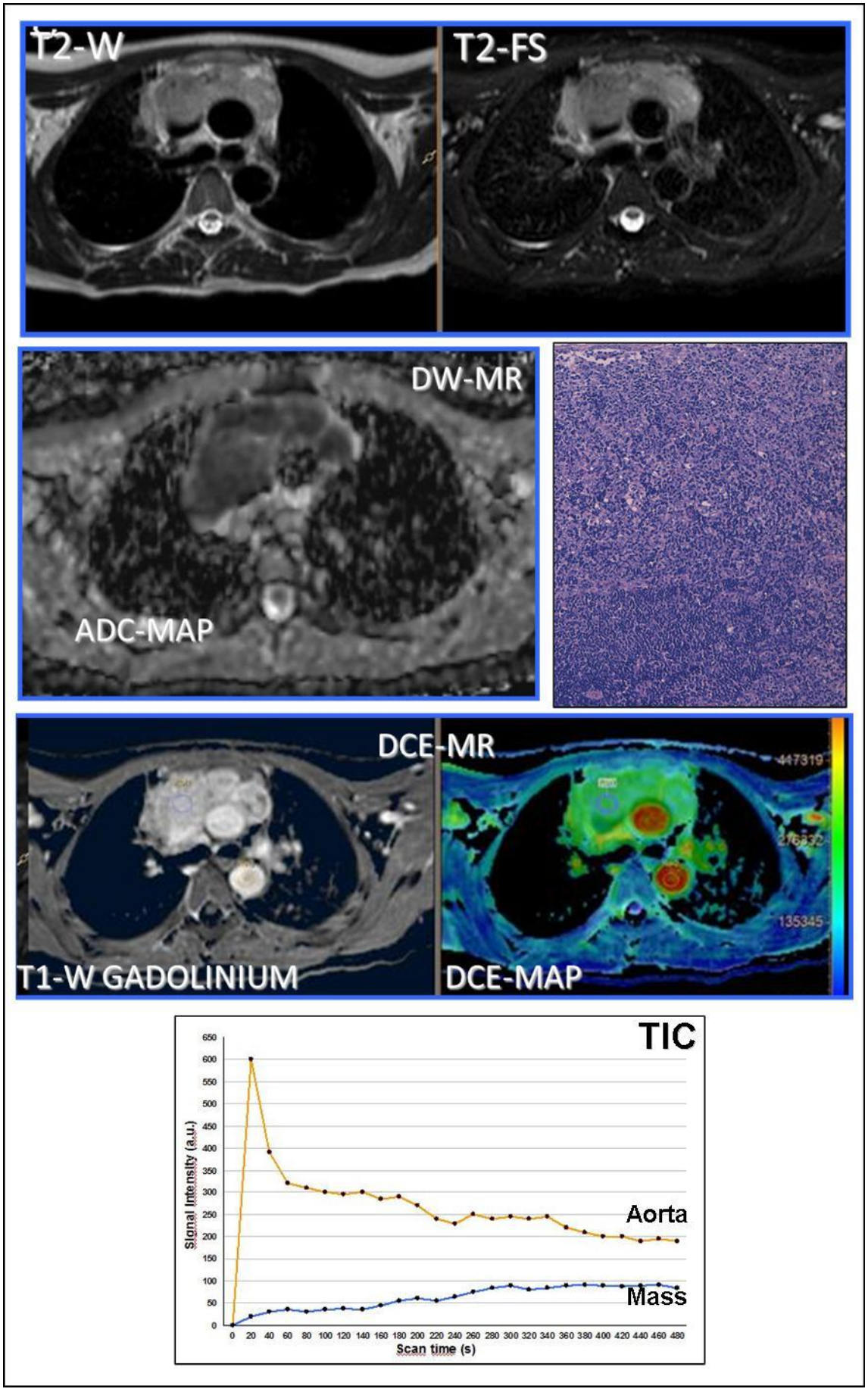
T2-W
T2-FS
DW-MR
ADC-MAP
DCE-MR
447319
276332
135345
T1-W GADOLINIUM
DCE-MAP
TIC
Signal Intensity (a.u.)
650
600
550
500
450
400
350
300
250
200
150
100
50
0
0 20 40 60 80 100 120 140 160 180 200 220 240 260 280 300 320 340 360 380 400 420 440 460 480
Scan time (s)
Aorta
Mass

Invasive (stage III, Masaoka-Koga staging system) high-grade (type B3, WHO classification system) thymoma in a 52-year-old man.

Transverse T2-weighted magnetic resonance images without (**T2-W**) and with fat suppression (**T2-FS**) show a large mass in the anterior mediastinum with soft tissue attenuation and inhomogeneous signal intensity. The signal intensity is higher compared to muscles in T2-W imaging.

Apparent diffusion coefficient map (**ADC-map)** of diffusion-weighted magnetic resonance imaging shows a low-signal intensity lesion for restricted diffusion to the water molecules movement, with ADC of $0.79x10^{-3}mm^2/s$.

Dynamic contrast-enhanced magnetic resonance (**DCE-MR**) shows a bulky mass in the anterior mediastinum, with diffuse low vascularisation, a low ratio compared to aorta, and a persistent pattern of the time-signal intensity curve (time to peak of 300s, wash out ratio less than 5%).

Photomicrograph of a representative histological section of thymoma, obtained after surgical removal, shows a tissue of high cellular density that is predominantly composed by medium-sized polygonal epithelial cells with mild atypia mixed with a limited component of lymphocytes (WHO type, B3). No fat cells are appreciable (Hematoxylin and eosin stain; original magnification, x100).